Geophysical Research Letters

RESEARCH LETTER
10.1029/2022GL100569

Key Points:

- Gravity waves were measured in the mesopause region before and during the current Southwestern North American megadrought
- Wave-driven temperature variance during the drought decreased by 28% and changed from primarily semiannual to primarily annual variations
- Decreased wave activity may be related to the summer and winter precipitation deficits during the ongoing megadrought

Supporting Information:

Supporting Information may be found in the online version of this article.

Correspondence to:

C. S. Gardner,
cgardner@illinois.edu

Citation:

Gardner, C. S., & She, C.-Y. (2022). Signature of the contemporary Southwestern North American megadrought in mesopause region wave activity. *Geophysical Research Letters*, *49*, e2022GL100569. https://doi.org/10.1029/2022GL100569

Received 24 JUL 2022
Accepted 27 SEP 2022

Author Contributions:

Conceptualization: Chester S. Gardner, Chiao-Yao She
Data curation: Chiao-Yao She
Formal analysis: Chester S. Gardner
Funding acquisition: Chester S. Gardner
Investigation: Chester S. Gardner
Methodology: Chester S. Gardner, Chiao-Yao She
Project Administration: Chester S. Gardner
Software: Chiao-Yao She
Validation: Chester S. Gardner, Chiao-Yao She

Signature of the Contemporary Southwestern North American Megadrought in Mesopause Region Wave Activity

Chester S. Gardner[1] and Chiao-Yao She[2]

[1]Department of Electrical & Computer Engineering, University of Illinois, Urbana, IL, USA, [2]Department of Physics, Colorado State University, Ft. Collins, CO, USA

Abstract The Southwestern North American megadrought began in 2000 and is now believed to be the driest 22-year period in the region since 800 CE. The precipitation deficit during the megadrought (8.3% during 2000–2021) has been accompanied by a significant decrease in gravity waves observed in the upper atmosphere. Prior to the drought (1990–2000), the mean wave-driven temperature fluctuation variances, between 85 and 100 km at Albuquerque and Ft. Collins, were comparable (62.2 ± 5.3 K^2 and 60.5 ± 1.8 K^2, respectively), with the largest variances occurring during winter and summer storm seasons. During the first decade of the drought (2001–2010), wave activity above Ft. Collins decreased by 28 ± 3%, mostly above 94 km, and changed from primarily semiannual to primarily annual variations. These changes may be related to reduced wave generation by tropospheric storms during the megadrought and to an altered geographic distribution of precipitation events in the western and mid-western United States.

Plain Language Summary Storm systems in the lower atmosphere can generate waves that propagate into the upper atmosphere to the edge of space, where their amplitudes become very large in response to decreasing atmospheric density. These waves drive the global circulation of the upper atmosphere and can even affect satellite orbits and space weather. We used laser radar (lidar) instruments at Albuquerque, New Mexico and Ft. Collins, Colorado to measure the strength of waves in the upper atmosphere before and during the current Southwestern North American (SWNA) megadrought, which is now believed to be the driest 22-year period in the region during the past 1200 years. We found a significant reduction in the wave activity in the upper atmosphere during the drought, which is likely related to below-normal precipitation associated with weakened summer and winter storms throughout the SWNA area. These results are important because they demonstrate that regional changes in the lower atmosphere can also impact the upper atmosphere, and because they can be used to test and validate the next generation of regional, high-resolution, atmospheric computer models that can resolve the small-scale waves observed by the lidars.

1. Introduction

The Earth's atmosphere is a coupled system in which processes and constituents in one altitude region can affect the processes and constituents in another, sometimes significantly. For example, nitric oxide (NO) densities peak in the thermosphere, where NO is produced by energetic particle precipitation and photoionization. NO is then transported into the stratosphere by the mean circulation and vertical mixing where it can catalyze the destruction of stratospheric ozone and affect the dynamics of the region (Crutzen, 1970; Lary, 1997). Conversely, the absorption of solar radiation by water vapor in the troposphere and ozone in the stratosphere, excite tidal oscillations that propagate into the upper atmosphere, where their amplitudes become large in response to decreasing atmospheric density. When these tides are combined in the upper atmosphere with oscillations generated in situ by solar absorption by ozone and molecular oxygen, they have a significant impact on the wind, temperature, and density structure of the mesosphere and thermosphere (Hagan et al., 2003). In recent decades, much research has focused on assessing the more subtle impact of global climate change in the lower atmosphere, on the structure of the upper atmosphere. Roble and Dickinson (1989) used a global numerical model to examine the effect of trace gas emissions in the lower atmosphere on the structure of the mesosphere, thermosphere and ionosphere. Their results suggested that doubling the mixing ratios of the greenhouse gases CO_2 and CH_4, would cool the mesosphere and thermosphere by 10 and 50 K, respectively. Long-term observations acquired at numerous sites in both the northern and southern hemispheres by a variety of techniques, have reported cooling trends in the mesosphere ranging up to about −10 K/decade (Laštovička et al., 2006; Qian et al., 2019; She et al., 2009).

Writing – original draft: Chester S. Gardner
Writing – review & editing: Chester S. Gardner, Chiao-Yao She

In this paper we explore the impact of the current Southwestern North American (SWNA) megadrought on gravity wave activity observed with Na lidars in the mesopause region above Albuquerque, NM (35°N, 106.5°W) and Ft. Collins, CO (41°N, 105°W). The SWNA megadrought began in 2000 and is now believed to be the driest 22-year period in the region since at least 800 CE (Williams et al., 2020, 2022). Summer and winter precipitation have decreased appreciably during the megadrought. We show that the precipitation deficit has been accompanied by a significant decrease in the gravity wave activity observed in the upper mesosphere above Ft. Collins.

2. Features of the Contemporary Southwestern Megadrought

The severe depletion of soil moisture that characterizes intense drought is caused primarily by below-normal precipitation, which can be exacerbated by increased evaporation arising from a combination of low humidity, high temperatures, and excessive winds. The southwestern region of North America has experienced numerous, extended periods of extreme drought during the past 2000 years that have been identified by examining tree-ring, streamflow, and other paleoclimate datasets, and by hydrological modeling (Gangopadhyay et al., 2022; Williams et al., 2020). A megadrought is typically defined as a prolonged drought lasting two decades or longer. The contemporary SWNA megadrought is notable, not only for its length (22 years), but also for its severity and the large geographic area affected (30–45°N, 105–125°W), which extends from northern Mexico to the northern borders of Oregon and Wyoming and from the Pacific Coast to the eastern borders of Wyoming, Colorado, and New Mexico (see Figure 1 in Williams et al., 2022). The mean water-year (October–September) precipitation from 2000 to 2020 during the drought, was 8.3% below the 1950–1999 average for the SWNA region and the temperature was 0.91°C above average (Williams et al., 2022). The current megadrought is now considered to be the driest 22-year period since 800 CE. This drought is also unique in that its morphology appears to be somewhat different from the Medieval megadroughts which occurred relatively frequently in SWNA area before 1600 CE (Seager et al., 2007; Steiger et al., 2019). By examining anthropogenic trends in temperature, relative humidity, and precipitation predicted by 29 climate models, Williams et al. (2022) conclude that anthropogenic warming has made a significant contribution (∼42%) to the severity of the current megadrought.

We explore how the megadrought may have affected the gravity waves observed in the mesosphere above the SWNA region. Gravity waves are generated in the troposphere by airflow over irregular topography (orographic forcing) and by convection and frontogenesis associated with storm systems. They propagate upward while increasing in amplitude in response to decreasing atmospheric density. The SWNA region has two periods of appreciable precipitation during the year. Winter precipitation during November through March comes from storms originating in the Pacific Ocean. Summer precipitation during July, August, and September comes from monsoon rains that obtain their moisture primarily from the warm waters in the Gulf of California and the eastern Pacific Ocean off the coast of Mexico, and to a lesser extent from the Gulf of Mexico (Adams & Comrie, 1997). The influence of the monsoon on total annual precipitation depends on location. Eastern Arizona and much of New Mexico receive about half of their annual precipitation from monsoonal storms (Douglas et al., 1993; Higgins et al., 1997), although the strength of the monsoon varies from year to year (Adams & Comrie, 1997). The trends in precipitation have changed significantly during the current SWNA megadrought (*NOAA National Centers for Environmental Information* https://www.ncei.noaa.gov/access/monitoring/us-trends/prcp/ann, Figure S1 in Supporting Information S1). During winter the precipitation has declined noticeably over the Pacific northwest, most of California, southern Arizona, southern New Mexico, and eastern Texas. It has increased somewhat over Colorado, Wyoming, Montana and Idaho. During summer, precipitation has declined significantly throughout much of the mountain west and Texas, and over most of New Mexico and Colorado.

3. Observed Wave Activity 85–100 km Above Albuquerque and Ft. Collins

The intensity of gravity wave activity in the middle atmosphere-lower thermosphere (MLT) has been characterized by analyzing wind and temperature measurements made by a variety of radio and optical techniques (e.g., Chen et al., 2019; Ern et al., 2018; Hoffman et al., 2011; Jacobi, 2014). She et al. (2022) provides a summary of those previous observations. Although the seasonal variations of wave activity, as quantified by the variances of the wave-driven wind and temperature fluctuations, differ depending on location and altitude, most of the observations show that wave fluctuations are strongest, either during winter or during both winter and summer, and weakest during spring and fall. Thus, the seasonal variations in the MLT are dominated by either annual

oscillations (AO) or a combination of annual plus semi-annual oscillations (SAO) with the phases linked to the solstices and equinoxes. The cause of this seasonality is related to the wave sources in the troposphere and to the atmosphere through which the waves propagate to reach the MLT. An important source of waves in the SWNA region is convection and frontogenesis related to storm systems and their concomitant precipitation, which exhibit strong semi-annual variations (Douglas et al., 1993; Higgins et al., 1997). As the wave spectrum propagates upward into the MLT and grows in amplitude, it is affected by the mean wind and temperature structure. Some waves are blocked when they encounter critical layers, while others break when they become convectively or dynamically unstable. Because the horizontal wind and temperature profiles throughout the atmosphere also exhibit seasonal variations, the intensity of wave activity in the MLT is a complex combination of the seasonality of the wave sources in the troposphere and the seasonality of wave filtering above the sources.

In the late 1990s, a Na Doppler lidar, coupled to a large-aperture steerable telescope (3.5 m diameter), was used to make high resolution 3-D winds and temperature profile observations in the mesopause region above the Starfire Optical Range, NM (SOR, 35°N, 106.5°W) on the Kirtland Air Force Base near Albuquerque, NM (Gardner & Liu, 2007). The data were acquired at night (49 nights), on a campaign basis, from June 1998 to November 2000 during the 2-week periods surrounding new moon. Thus, the observations correspond largely to the period prior to the onset of the current SWNA megadrought. Data were acquired in every month but July. Persistent cloud cover accompanying the summer monsoon storms, prevented data acquisition in July during all 3 years of the campaign.

The complexity of the seasonal variations of the wave-driven wind and temperature variance profiles at SOR is illustrated in Figures 4 and 5 of Gardner and Liu (2007). These data include the effects of gravity waves with vertical wavelengths between 1 and ∼20 km, the mean altitude range of observations (∼83–103 km) and observed wave periods between 3 min and ∼7.5 hr, the mean duration of the nighttime measurement periods. The annual means plus the 12-month (AO) and 6-month (SAO) harmonic fits to the measured fluctuation variances (Table S1 in Supporting Information S1) are plotted versus month in Figure 1. The harmonic fit parameters are summarized in Table 1. For the horizontal wind and temperature variances, the SAO amplitudes are more than double the AO amplitudes, while for the vertical wind variance the AO amplitude is largest. In all cases the wave-driven fluctuation variances are strongest in the winter and summer following the solstices and weakest in the spring and fall.

Beginning in March 1990 and continuing until March 2010, a Na Doppler lidar was also operated at Colorado State University (CSU, 41°N, 105°W) in Ft. Collins, CO to make measurements of temperature, Na density, and radial winds in the mesopause region (She & Yu, 1994; She et al., 1990). Detailed descriptions of this extensive data set and how it was processed can be found in the CSU temperature and gravity wave trend and climatology papers (She et al., 2009, 2019, 2022). The nighttime data were divided into two subsets, one comprising measurements acquired before 2001 (479 nights), roughly corresponding to the period prior to the onset of the megadrought, and another for measurements acquired from January 2001 through March 2010 (477 nights), corresponding to the first 10 years of the megadrought. The temperature variances derived from both subsets, include the effects of gravity waves with vertical wavelengths between 3 and ∼20 km and observed wave periods between 20 min and ∼8.2 hr (Gardner et al., 2022; She et al., 2022). Because of the large number of observations, both before and during the drought, it was possible to characterize the seasonal variations of wave activity at CSU with a high degree of precision. Furthermore, by averaging 10-year of data, the impact of the 11-year solar cycle on wave activity is largely eliminated (e.g., Ern et al., 2011; Jacobi, 2014; Liu et al., 2017).

The monthly mean fluctuation variances between 85 and 100 km at CSU (Table S1 in Supporting Information S1) are plotted versus month in Figure 1d along with the 12-month plus 6-month harmonic fits to the measured data (Table 1). Like the SOR data, the CSU data (1990–2000) prior to the megadrought is dominated by the SAO with the strongest wave activity in winter and summer following the solstices and weakest in spring and fall. The seasonal variations are quite similar (see Figure 1c) and the annual mean temperature variances (85–100 km) are nearly identical at the two sites (62.2 ± 5.3 K^2 @ SOR and 60.5 ± 1.8 K^2 @ CSU). During the first 10 years of the megadrought the annual mean temperature variance at CSU decreased by 28 ± 3% to 43.4 ± 1.3 K^2 while the AO dominated the seasonal variations.

The seasonal variations of the CSU data during the initial 10 years of the drought are dramatically different from the SOR and CSU data prior to the drought. During the drought the mean temperature variance at CSU is smaller at all times of the year and most significantly during summer (June, July, and August), where the total variance

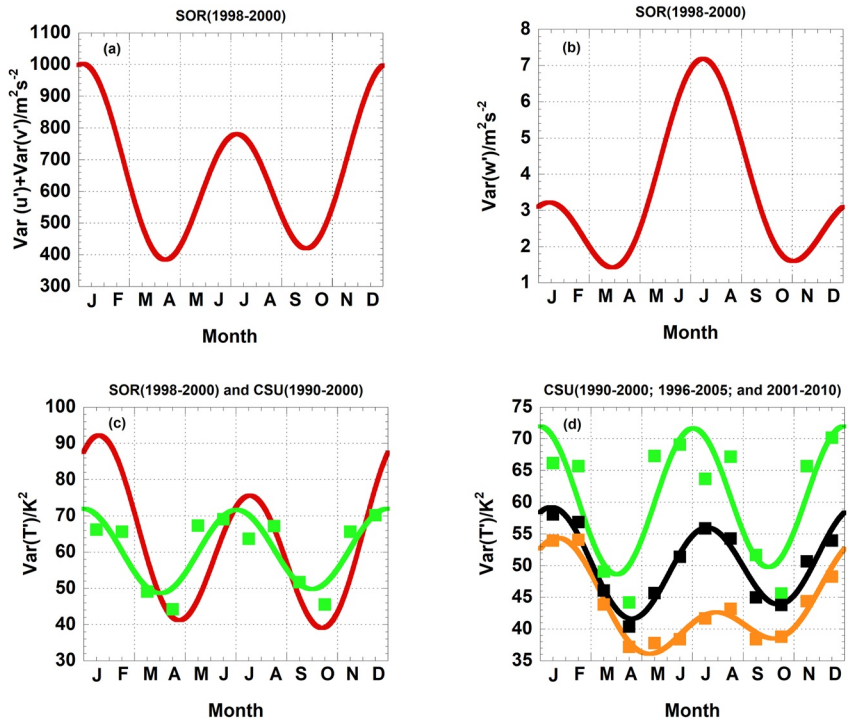

Figure 1. Seasonal variations of the mean fluctuation variances between 85 and 100 km. (a) Horizontal wind variance at Starfire Optical Range (SOR) (1998–2000), (b) vertical wind variance at SOR (1998–2000), and (c) temperature variance at SOR (1998–2000, red curve) and at CSU (1990–2000, green curve), all observed prior to the onset of the current SWNA megadrought. (d) Temperature variance at CSU before (1990–2000, green curve) and during (2001–2010, brown curve) the megadrought and during the transition period (1996–2005, black curve). The symbols are the monthly means (Table S1 in Supporting Information S1), and the smooth curves are the mean plus annual oscillations and semi-annual oscillations harmonic fits to the data (Table 1).

decreased by 38 ± 5% to about 41.1 ± 2.5 K^2 compared to 66.7 ± 4 K^2 at CSU and 65.9 ± 16 K^2 at SOR prior to the drought (Table S1 in Supporting Information S1). While semiannual oscillations are prominent at SOR and CSU prior to the drought, the SAO amplitude is much weaker at CSU during the drought. The annual mean (A_M), AO amplitude (A_{AO}), and SAO amplitude (A_{SAO}) profiles are plotted in Figure 2. Although the annual mean profile is smaller at all altitudes during the drought, the most significant changes occur above 94 km. At the higher altitudes, the variance remained essentially constant with altitude at ~38 K^2 during the drought, while before the drought, the variance increased rapidly with increasing altitude exceeding 100 K^2 at 100 km. The AO amplitude profiles before and during the drought are comparable. The SAO amplitude is quite prominent before the drought at all altitudes, but is much weaker during the drought, except for a narrow altitude range near 87 km. Above 90 km the SAO amplitude before the drought increases with increasing altitude reaching a maximum value

Table 1
Parameters of the Mean Plus Annual and Semiannual Harmonic Fits to the Measured Fluctuation Variances

Harmonic model = $A_M + A_{AO}\cos\left[\frac{2\pi}{12}(m - m_{AO})\right] + A_{SAO}\cos\left[\frac{2\pi}{6}(m - m_{SAO})\right]$

Site (period)	Parameter	Model uncertainty	A_M annual mean	A_{AO}	m_{AO} (mo)	A_{SAO}	m_{SAO} (mo)
SOR (June 1998–November 2000)	Var(u') + Var(v')	±125 m^2s^{-2}	650 ± 55 m^2s^{-2}	113 m^2s^{-2}	−0.12	241 m^2s^{-2}	0.20
	Var(w')	±1.3 m^2s^{-2}	3.5 ± 0.6 m^2s^{-2}	2.0 m^2s^{-2}	6.6	1.6 m^2s^{-2}	0.47
	Var(T')	±12 K^2	62.2 ± 5.3 K^2	8.3 K^2	0.82	21.8 K^2	0.58
CSU (1990–2000)	Var(T')	±4.0 K^2	60.5 ± 1.8 K^2	0.59 K^2	−2.52	11.3 K^2	0.01
CSU (1996–2005)	Var(T')	±3.5 K^2	52.2 ± 1.6 K^2	1.98 K^2	−0.66	7.39 K^2	0.51
CSU (2001–2010)	Var(T')	±2.9 K^2	43.4 ± 1.3 K^2	6.1 K^2	0.40	5.1 K^2	0.79

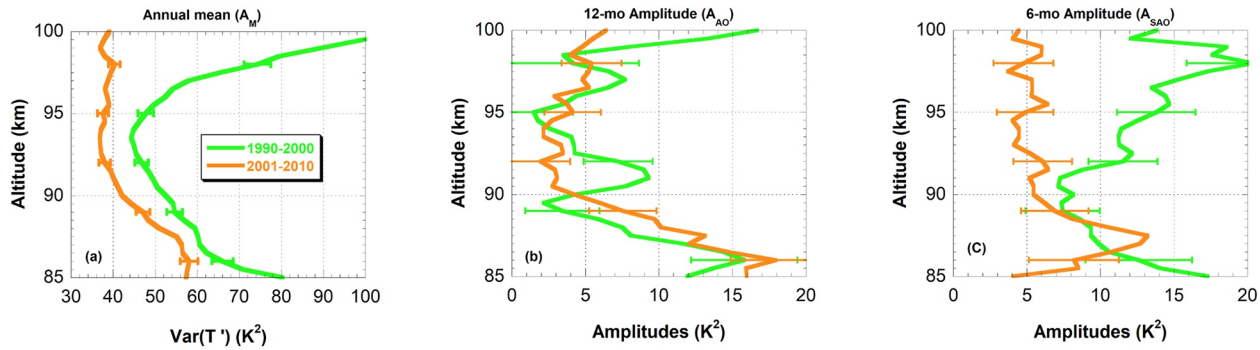

Figure 2. Profiles of the (a) annual mean (A_M), (b) 12-month amplitude (A_{AO}), and (c) 6-month amplitude (A_{SAO}) of the harmonic fits to the temperature fluctuation variance observed at CSU prior to the current SWNA megadrought (1990–2000, green curves) and during the first 10 years of the megadrought (2001–2010, brown curves). The error bars represent the rms uncertainties in the derived harmonic fit parameters. The plots were derived from the monthly mean Var(T') profiles (Tables S2 and S4 in Supporting Information S1).

of 20 K^2 at 98 km compared to just 5 K^2 at this same altitude during the drought. These results are statistically significant, as indicated by the error bars included on the profiles.

Additional insight about the seasonal variations can be obtained by examining the seasonal mean temperature variance profiles plotted in Figure 3. The largest seasonal difference occurs in summer (June, July, August, Figure 3c), which is probably related to reduced precipitation associated with a weaker summer monsoon. However, the mean temperature variance decreased in all seasons during the drought ($-23 \pm 7\%$ in winter, $-26 \pm 6\%$ in spring, $-38 \pm 5\%$ in summer, and $-25 \pm 6\%$ in fall). The decreases are largely concentrated above

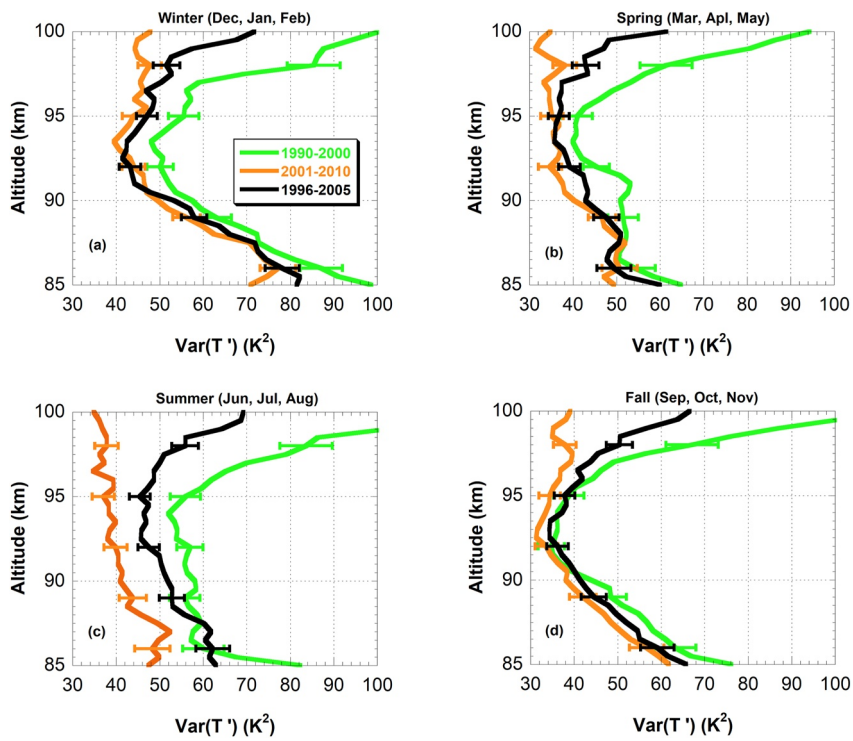

Figure 3. Profiles of the temperature fluctuations variances observed during (a) winter (December, January, February), (b) spring (March, April, May), (c) summer (June, July, August), and (d) fall (September, October, November) observed at CSU prior to current southwestern north american (SWNA) megadrought (1990–2000, green curves), during the first 10 years of the drought (2001–2010, brown curves) and during the transition period (1996–2005, black curves). The error bars represent the rms uncertainties in the derived profiles. The plots were derived from the monthly mean Var(T') profiles (Tables S2, S3, and S4 in Supporting Information S1).

94 km. Potential causes of this behavior are discussed in the following section. To provide insight on the changing wave activity during the drought transition, the seasonal variations and profiles of Var(T') were computed using CSU data acquired during 1996–2005. The results are plotted as black curves in Figures 1d and 3. The transition curves fall roughly midway between the curves derived from data acquired prior to the drought and during the first 10 years of the drought.

4. Discussion

Both SOR and CSU are mid-latitude mountain sites located in the eastern portion of the SWNA region, with SOR situated about 625 km south-southwest of CSU. The waves observed at mesopause heights above both sites include a mixture of mountain and storm-generated waves. A large fraction (but not all) of these waves originated within the megadrought region. The geographic extent of the lower-atmosphere wave sources can be estimated by applying gravity wave theory. Gravity waves are partially polarized transverse waves with the degree of polarization dependent on their intrinsic frequencies (ω). Low-frequency waves with ω near the inertial frequency (f) are nearly circularly polarized and high-frequency waves with ω near the buoyancy frequency (N) are nearly linearly polarized. Because the waves observed at SOR and CSU had periods much smaller than the inertial periods ($\lesssim$7.5 vs. 20.9 hr @ SOR, $\lesssim$8.2 vs. 18.4 hr @ CSU), the wave fields were largely linearly polarized. Therefore, according to the gravity wave polarization relations (Vadas, 2013), for these high frequency waves the vertical and horizontal wind amplitudes (w' = vertical, u' = zonal, and v' = meridional) and wavelengths (λ_z = vertical and λ_h = horizontal) are related as follows

$$\frac{|w'|}{\sqrt{(u')^2+(v')^2}} \simeq \frac{\lambda_z}{\lambda_h} \tag{1}$$

In the absence of refraction and ducting (which assumes zero background wind), a wave generated near the tropopause would propagate upward at an elevation angle approximately equal to $\tan^{-1}(\lambda_z/\lambda_h) \simeq \tan^{-1}\left(|w'|/\sqrt{(u')^2+(v')^2}\right)$. By using the SOR wind data (Figure 4 in Gardner & Liu, 2007), we find that the wave field observed in the mesopause region, originated near the tropopause, nominally within a circular region centered at SOR with a radius of ~1450 km in winter (December, January, February) and ~850 km in summer (June, July, August). Thus, for SOR, approximately half the waves observed at mesopause heights originated within the SWNA region. Notice that the significant increase in the vertical wind variance during summer, illustrated in Figure 1b, arises in part because the waves are generated closer to SOR and therefore are propagating more vertically in summer compared to winter.

Unfortunately, we are unable to make similar estimates for the CSU site because the CSU lidar did not measure the vertical wind. But, if these same radii also apply approximately to CSU, then some of the waves observed at CSU would have originated outside the SWNA region as far east as eastern Kansas and Nebraska in summer and Illinois in winter, and as far north as central Montana in summer and southern Saskatchewan in winter. However, like the SWNA area, these eastern and northern regions also experienced significant decreases in precipitation during summer from 1990 to 2020 (Figure S1 in Supporting Information S1). Furthermore, in winter the reduced wave generation in the much drier regions in California, southern Arizona, southern New Mexico and Texas likely outweigh the increased wave generation in the moderately wetter regions in Colorado, Wyoming, Montana, and Idaho. Thus, we expect a decrease in waves generated by tropospheric convection and frontogenesis during both summer and winter over these areas. The global momentum flux observations reported by Ern et al. (2018, Figures 13f–13h and 14f–14h) also exhibit very strong wave activity over North America during summer (June, July, August), which is likely caused by convective sources that would be affected by reduced precipitation during the drought.

Enhanced dissipation of waves in the middle atmosphere, caused by changes in the background wind and temperature structure, could potentially be responsible for the significant decrease in the temperature variance observed above 94 km for all seasons at CSU during the 2001–2010 period (see Figure 3). But, because the background structure of the middle atmosphere is driven largely by global processes, enhanced dissipation, if it occurred, is unlikely to be related to the SWNA megadrought, which is a local/regional phenomenon. However, changes in the strength and number of the wave sources and their geographic distribution during the drought may play important

roles. The SOR data show that the largest vertical wind variance occurs during summer below 94 km where it averages about 8.5 m^2s^{-2} compared to about 500 m^2s^{-2} for the horizontal wind variance (Figure 4, Gardner & Liu, 2007). Thus, the waves in this lower altitude range probably originated even closer to Albuquerque during summer (within ~600 km), and could be dominated by mountain waves generated by airflow over the local topography, while the waves above 94 km, originated farther away (~1,000 km). These distances are just rough estimates because we have neglected the potential impact of wave refraction and ducting by the background winds. Furthermore, some primary waves could break at lower altitudes and generate secondary waves that would have their origin above the tropopause, much closer to Albuquerque (Vadas & Becker, 2018; Vadas et al., 2018). Even so, the SOR data provide qualitative support for the notion that the geographic distribution of tropospheric wave sources, as well as their number and strength, can affect the profile of wave-driven temperature fluctuations in the upper atmosphere. The annual mean vertical and horizontal wind variances at SOR above 94 km before the drought are ~3 and ~750 m^2s^{-2}, respectively, which corresponds to a tropospheric origin within ~1,400 km of Albuquerque. These waves could have originated as far west as the Sierra Nevada Mountains in California, as far east as Missouri, Arkansas, and Texas, and as far north as Montana. We speculate that the significant decrease in temperature variance above 94 km throughout the year at CSU during the drought is probably related to a significant decrease in these most distant waves sources, especially those sources within the SWNA region. It's possible that the temperature fluctuations below 94 km at CSU are dominated by locally generated mountain waves, which did not change much during the drought, while the fluctuations above 94 km are dominated by more distant storm-generated waves, which did change appreciably during the drought.

5. Conclusions

We acknowledge that attributing changes in MLT wave activity during the current megadrought, to a reduction in the number and strength of waves generated by the storm systems and frontogenesis associated with the reduced precipitation in the SWNA region, is speculative, but it is physically plausible. However, changes in the geographic distribution of waves sources and the environment through which the waves propagate, must also play important roles in reducing the wave activity measured in the upper atmosphere. This includes changes in filtering, refracting, ducting, and dissipation of the waves by the background winds. To fully assess the importance of all these processes, requires analysis with a high-resolution, regional computer model that can resolve the small-scale gravity waves observed by the Na Doppler lidars used for this current study.

In summary, the intensity and seasonal variations of the mesopause region wave activity observed at SOR and CSU prior to the current megadrought are quite similar. Semiannual oscillations dominate the temperature fluctuation variances, and the annual mean variances are nearly identical. During the first 10 years of the drought, the CSU wave activity changed significantly. The annual mean temperature variance decreased by 28 ± 3%, and annual oscillations, rather than semiannual oscillations, dominated the seasonal variations. The decline in wave activity was most significant in summer and above 94 km during all seasons. We suggest that these changes may be related to the precipitation deficit during the megadrought and perhaps to an altered geographic distribution of precipitation events in the western and mid-western United States.

Data Availability Statement

The nightly mean and high-resolution CSU Na lidar temperature data (1990–2010) are available from Madrigal Database at Millstone Hill (http://millstonehill.haystack.mit.edu/) and from the Digital Commons of Utah State University (Yuan, 2021, https://doi.org/10.15142/T33H26). The monthly mean Var(T') profiles at CSU for the three 10-year periods studied were obtained from She et al. (2022) and are provided in the Supporting Information. The Starfire Optical Range Na lidar data were obtained from the tables and figures published in Gardner and Liu (2007).

Acknowledgments
The authors acknowledge with great appreciation the contributions of former students and post-doctoral researchers who participated in the Na lidar data acquisition at CSU and SOR. We thank Dr. Zhao-Ai Yan at the National Space Science Center of the Chinese Academy of Sciences for his help in preparing the figures. We also thank two anonymous reviewers for their constructive suggestions for clarifying the data interpretation. This work was supported in part by National Science Foundation Grant AGS-2029162.

References

Adams, D. K., & Comrie, A. C. (1997). The North American monsoon. *Bulletin of the American Meteorological Society*, *78*(10), 2197–2214. https://doi.org/10.1175/1520-0477(1997)078<2197:TNAM>2.0.CO;2

Chen, D., Strube, C., Ern, M., Preusse, P., & Riese, M. (2019). Global analysis for periodic variations in gravity wave squared amplitudes and momentum fluxes in the middle atmosphere. *Annales de Geophysique*, *37*(4), 487–506. https://doi.org/10.5194/angeo-37-487-2019

Crutzen, P. J. (1970). The influence of nitrogen oxides on the atmospheric ozone content. *Quarterly Journal of the Royal Meteorological Society*, *96*(408), 320–325. https://doi.org/10.1002/qj.49709640815

Douglas, M. W., Maddox, R., Howard, K., & Reyes, S. (1993). The Mexican monsoon. *Journal of Climate*, *6*(8), 1665–1667. https://doi.org/10.1175/1520-0442(1993)006<1665:TMM>2.0.CO;2

Ern, M., Preusse, P., Gille, J. C., Hepplewhite, C. L., Mlynczak, M. G., Russell, J. M., III, & Riese, M. (2011). Implications for atmospheric dynamics derived from global observations of gravity wave momentum flux in stratosphere and mesosphere. *Journal of Geophysical Research*, *116*(D19), D19107. https://doi.org/10.1029/2011JD015821

Ern, M., Trinh, Q. T., Preusse, P., Gille, J. C., Mlynczak, M. G., Russell, J. M., III, & Riese, M. (2018). Gracile: A comprehensive climatology of atmospheric gravity wave parameters based on satellite limb soundings. *Earth System Science Data*, *10*(2), 857–892. https://doi.org/10.5194/essd-10-857-2018

Gangopadhyay, S., Woodhouse, C. A., McCabe, G. J., Routson, C. C., & Meko, D. M. (2022). Tree rings reveal unmatched 2nd century drought in the Colorado River Basin. *Geophysical Research Letters*, *49*(11), e2022GL098781. https://doi.org/10.1029/2022GL098781

Gardner, C. S., & Liu, A. Z. (2007). Seasonal variations of the vertical fluxes of heat and horizontal momentum in the mesopause region at Starfire Optical Range, New Mexico. *Journal of Geophysical Research*, *112*(D9), D09113. https://doi.org/10.1029/2005JD006179

Gardner, C. S., She, C.-Y., & Yan, Z.-A. (2022). Seasonal variations of gravity wave induced thermal and constituent diffusivities in the mesopause region above Ft. Collins, CO (40.6°N, 105.1°W). *Journal of Geophysical Research: Atmospheres*, *127*(11), e2021JD036387. https://doi.org/10.1029/2021JD036387

Hagan, M. E., Forbes, J. M., & Richmond, A. D. (2003). In J. R. Holton (Ed.), *Atmospheric tides, encyclopedia of atmospheric sciences* (pp. 159–165). Academic Press. ISBN9780122270901. https://doi.org/10.1016/B0-12-227090-8/00409-7

Higgins, R. W., Yao, Y., & Wang, X. L. (1997). Influence of the North American monsoon system on the U.S. summer precipitation regime. *Journal of Climate*, *10*(10), 2600–2622. https://doi.org/10.1175/1520-0442(1997)010<2600:IOTNAM>2.0.CO;2

Hoffmann, P., Rapp, M., Singer, W., & Keuer, D. (2011). Trends of mesospheric gravity waves at northern middle latitudes during summer. *Journal of Geophysical Research*, *116*, D00P08. https://doi.org/10.1029/2011JD015717

Jacobi, C. (2014). Long-term trends and decadal variability of upper mesosphere/lower thermosphere gravity waves at midlatitudes. *Journal of Atmospheric and Solar-Terrestrial Physics*, *118*, 90–95. https://doi.org/10.1016/j.jastp.2013.05.009

Lary, D. J. (1997). Catalytic destruction of stratospheric ozone. *Journal of Geophysical Research*, *102*(D17), 21515–21526. https://doi.org/10.1029/97JD00912

Laštovička, J., Akmaev, R. A., Beig, G., Bremer, J., & Emmert, J. T. (2006). Global change in the upper atmosphere. *Science*, *314*(5803), 1253–1254. https://doi.org/10.1126/science.1135

Liu, X., Yue, J., Xu, J., Garcia, R. R., Russell, J. M., III, Mlynczak, M., et al. (2017). Variations of global gravity waves derived from 14 years of SABER temperature observations. *Journal of Geophysical Research: Atmospheres*, *122*(12), 6231–6249. https://doi.org/10.1002/2017JD026604

Qian, L., Jacobi, C., & McInerney, J. (2019). Trends and solar irradiance effects in the mesosphere. *Journal of Geophysical Research: Space Physics*, *124*(2), 1343–1360. https://doi.org/10.1029/2018JA026367

Roble, R. G., & Dickinson, R. E. (1989). How will changes in carbon dioxide and methane modify the mean structure of the mesosphere and lower thermosphere? *Geophysical Research Letters*, *16*(12), 1441–1444. https://doi.org/10.1029/GL016i012p01441

Seager, R., Graham, N., Herweijer, C., Gordon, A. L., Kushnir, Y., & Cook, E. (2007). Blueprints for medieval hydroclimate. *Quaternary Science Reviews*, *26*(19–21), 2322–2336. https://doi.org/10.1016/j.quascirev.2007.04.020

She, C. Y., Berger, U., Yan, Z.-A., Yuan, T., Lübken, F.-J., Krueger, D. A., & Hu, X. (2019). Solar response and long-term trend of midlatitude mesopause region temperature based on 28 Years (1990–2017) of Na lidar observations. *Journal of Geophysical Research: Space Physics*, *124*(8), 7140–7156. https://doi.org/10.1029/2019JA026759

She, C.-Y., Krueger, D. A., Akmaev, R., Schmidt, H., Talaat, E., & Yee, S. (2009). Long-term variability in mesopause region temperatures over Fort Collins, CO (41°N, 105°W) based on lidar observations from 1990 through 2007. *Journal of Atmospheric and Solar-Terrestrial Physics*, *71*(14–15), 1558–1564. https://doi.org/10.1016/j.jastp.2009.05.007

She, C. Y., Latifi, H., Yu, J. R., Alvarez, R. J., Bills, R. E., & Gardner, C. S. (1990). Two-frequency lidar technique for mesospheric Na temperature measurements. *Geophysical Research Letters*, *17*(7), 929–932. https://doi.org/10.1029/gl017i007p00929

She, C.-Y., Yan, Z.-A., Gardner, C. S., Krueger, D. A., & Hu, X. (2022). Climatology and seasonal variations of temperatures and gravity wave activities in the mesopause region above Ft. Collins, CO (40.6°N, 105.1°W). *Journal of Geophysical Research: Atmospheres*, *127*(11), e2021JD036291. https://doi.org/10.1029/2021JD036291

She, C.-Y., & Yu, J. R. (1994). Simultaneous three-frequency Na lidar measurements of radial wind and temperature in the mesopause region. *Geophysical Research Letters*, *21*(17), 1771–1774. https://doi.org/10.1029/94gl01417

Steiger, N. J., Smerdon, J. E., Cook, B. I., Seager, R., Williams, A. P., & Cook, E. R. (2019). Oceanic and radiative forcing of medieval megadroughts in the American Southwest. *Science Advances*, *5*(7), eaax0087. https://doi.org/10.1126/sciadv.aax00

Vadas, S. L. (2013). Compressible f-plane solutions to body forces, heatings, and coolings, and application to the primary and secondary gravity waves generated by a deep convective plume. *Journal of Geophysical Research: Space Physics*, *118*(5), 2377–2397. https://doi.org/10.1002/jgra.50163

Vadas, S. L., & Becker, E. (2018). Numerical modeling of the excitation, propagation, and dissipation of primary and secondary gravity waves during wintertime at McMurdo Station in the Antarctic. *Journal of Geophysical Research: Atmospheres*, *123*(17), 9326–9369. https://doi.org/10.1029/2017JD027974

Vadas, S. L., Zhao, J., Chu, X., & Becker, E. (2018). The excitation of secondary gravity waves from local body forces: Theory and observation. *Journal of Geophysical Research: Atmospheres*, *123*(17), 9296–9325. https://doi.org/10.1029/2017JD027970

Williams, A. P., Cook, B. I., & Smerdon, J. E. (2022). Rapid intensification of the emerging southwestern North American megadrought in 2020–2021. *Nature Climate Change*, *12*(3), 232–234. https://doi.org/10.1038/s41558-022-01290-z

Williams, A. P., Cook, E. R., Smerdon, J. E., Cook, B. I., Abatzoglou, J. T., Bolles, K., et al. (2020). Large contribution from anthropogenic warming to an emerging North American megadrought. *Science*, *368*(6488), 314–318. https://doi.org/10.1126/science.aaz9600

Yuan, T. (2021). *USU-CSU Na lidar data*. Utah State University Digital Commons. https://doi.org/10.15142/T33H26